J Opt (December 2018) 47(4):481–488
https://doi.org/10.1007/s12596-018-0482-x

RESEARCH ARTICLE

Investigation on chirping characteristics of a 1.55-µm directly modulated distributed feedback laser

Abida Yousuf[1] · **Hakim Najeeb-ud-din**[1]

Received: 5 October 2017 / Accepted: 16 August 2018 / Published online: 8 September 2018

Abstract We investigate the laser chirp characteristics of a 1.55-µm directly modulated DFB laser by simulation. The chirp is characterized by two important parameters: gain compression and α-factor. Measurements of the chirp parameters using transfer function and the chirp-to-modulated power ratio are presented here. We have identified that the characteristic frequency (f_c) represents the boundary between the adiabatic and transient chirp, i.e., the adiabatic chirp dominates for $f < f_c$ and the transient chirp dominates for $f > f_c$. Frequency excursion for both chirp terms is well characterized by the phase rate equation model that describes the chirping behavior, switching transients and the power overshoots. Finally, proper adiabatic chirp is generated by adjusting: the laser device parameters and the operating conditions to achieve dispersion-tolerant system.

Keywords Distributed feedback laser (DFB) · Chirping (adiabatic and transient) · Chirp-to-modulated power ratio (CPR) · Gain compression · α-Factor

Introduction

Understanding the difficulties that limit the high-speed modulation of directly modulated lasers is crucial to the development of semiconductor distributed feedback (DFB) lasers. Direct modulation is an attractive low-cost optical transmission scheme for optical access networks [1–3]. However, when the laser diode is modulated in several GHz range, a parasitic frequency modulation (chirping) is observed, and the maximum achievable transmission data rate is limited. Directly modulated lasers are classified according to their chirping behavior as adiabatic and transient, depending on the device design parameters and the driving conditions involved [4]. In such systems, the interaction of the laser chirp with chromatic dispersion of standard optical fiber limits maximum fiber length. Several studies have been reported to overcome the influence of laser originating nonlinearities. These include use of negative dispersion fibers or post-compensation techniques to enhance the transmission distance [5–8], feed-forward and predistortion precompensation techniques [9] and injection locking [10]. The primary parameters for characterizing the chirp in a directly modulated laser are linewidth enhancement factor (α) [11, 12] and the gain compression factor (ε) [13–15]. The gain compression parameter is important in describing the relation between the AM and FM behavior of laser diodes and is the dominant effect that introduces damping in the intensity modulation, which reduces the transient chirp and introduces the adiabatic chirp [16]. This phenomenon limits the modulation dynamics of directly modulated lasers through the adiabatic chirp and is responsible for the bending of the light–current characteristics. The α-factor is another most important parameter in describing the coupling between the intensity and frequency modulation of the laser diode. The α-factor influences several other fundamental aspects of semiconductor lasers, such as linewidth, laser behavior with respect to optical feedback, and in predicting the correlation between intensity and frequency noise [4]. The transient chirp is complicated by the fact that the disruption in phase and gain in the laser excite the natural resonance (relaxation oscillation) within the laser. There is significant loss of

✉ Abida Yousuf
abidayousuf_07phd13@nitsri.net

[1] Electronics and Communication Department, National Institute of Technology, Srinagar, India

energy during transient. When the laser stabilizes in the new bias condition, it is usually at a different frequency. This frequency shift corresponding to the low-frequency shift or adiabatic chirp related to the frequency offset between the On and Off levels during modulation.

The aim of this study is to characterize chirp parameters (gain compression and α-factor) in a directly modulated laser. This paper gives an overview of the measurement technique to characterize chirping effect. This work focuses on the intensity modulation (IM) accompanying frequency modulation (FM) behavior, and the large signal switching transients. We have identified that the characteristic frequency (f_c) represents the boundary between the adiabatic and transient chirp. The paper is organized as follows: Sect. 2 represents the laser model based on the single-mode laser rate equation. Section 3 represents frequency modulation (FM) which accompanies the desired intensity modulation (IM) at the output of the laser, addressing the significance of amplitudes of the sidebands of optical spectrum, to measure the FM and IM components at the laser output. Section 4 characterizes the chirp using transfer function and the chirp-to-modulated power ratio. Section 5 represents large signal switching transients based on the peak power overshoot are also addressed. Finally, the generation of proper chirp in a directly modulated DFB laser is realized by adjusting laser parameters and the operating conditions to achieve higher dispersion tolerance.

Laser rate equation

The modulation dynamics of the laser are modeled by coupled laser rate equations which describe the relation between the photon, electron density and the optical phase as [17]

$$\frac{dN(t)}{dt} = \frac{I(t)}{qV} - \frac{N(t)}{\tau_n} - v_g g_0 \frac{N(t) - N_t}{1 + \varepsilon S(t)} S(t) \tag{1}$$

$$\frac{dS(t)}{dt} = \left\{ \Gamma v_g g_0 \frac{N(t) - N_t}{1 + \varepsilon S(t)} - \frac{1}{\tau_p} \right\} S(t) + \frac{\Gamma \beta N(t)}{\tau_n} \tag{2}$$

$$\frac{d\phi(t)}{dt} = \frac{\alpha}{2} \left[\Gamma v_g g_0 (N(t) - N_t) - \frac{1}{\tau_p} \right] \tag{3}$$

where $N(t)$ is the carrier density (cm^{-3}), $S(t)$ is the photon density, $I(t)$ is the current injected into the active layer, q is the electron charge, β *is* the fraction of spontaneous emission coupled into the lasing mode, g_0 is the differential gain (cm^2), N_t is the electron density (cm^{-3}) at which net gain is zero, Γ is the optical confinement factor given by the ratio of the active region volume to the modal volume, τ_p is the photon lifetime (s) associated with cavity loss, τ_n is the carrier lifetime (s), ε is the gain compression coefficient, and V is the volume of the active layer (cm^3). The parameter ε (with units of volume) specifies the gain compression characteristics of the active region. Typically, the gain compression is small, but it has a dramatic effect on the dynamic response of the laser. A Runge–Kutta algorithm is used to numerically integrate the coupled first-order differential laser rate equations with noise and phase noise being disabled, and these equations apply to a noiseless laser oscillating in a single longitudinal mode above threshold. The photon and electron densities within the active region of the laser are assumed to be uniform. If parameter noise is enabled, the langevin noise terms for photon and electron densities are included in the model. If phase noise is enabled, the langevin noise term for the phase is included in the model [18]. Parameters *bias current* and *modulation peak current* are scale factors applied to the input electrical signal. The optical power $P(t)$ of the semiconductor laser to the injected current is determined from Eqs. (1)–(3) and is given as:

$$P(t) = \frac{V \eta h v}{2 \Gamma \tau_p} S(t) \tag{4}$$

where η is the differential quantum efficiency, h is planks constant, and v is the unmodulated optical frequency.

Simultaneous FM and IM modulation

The modulation of the carrier density modulates the gain, it also modulates the index of the active region. As a result, the optical length of the cavity is modulated by the current, causing the resonant mode to shift back and forth in frequency. The intensity of the simultaneous FM and IM modulated wave at the laser output can be expressed as [19].

$$I = I_0[1 + m\cos(2\pi f_m t)] \cdot \exp[j(2\pi f_0 t + \beta \sin(2\pi f_m t))] \tag{5}$$

where m and β are amplitude and frequency modulation indices respectively, f_m is the modulation frequency, and f_0 is the center frequency. On expanding Eq. (5) in terms of bessel function, the magnitude of carrier and its first sideband are:

Carrier:

$$I_C = I_0[j_0 \exp(j(2\pi f_0 t))] \tag{6}$$

Lower side band:

$$I_{-1} = I_0[-j_1(\beta) + (m/2)\{J_2(\beta) + J_0(\beta)\}] \exp(j(2\pi(f_0 - f_m)t)) \tag{7}$$

Upper sideband:

$$I_{+1} = I_0[j_1(\beta) + (m/2)\{J_2(\beta) + J_0(\beta)\}]\exp(j(2\pi(f_0 + f_m)t)) \quad (8)$$

The optical output power spectrum shown in Fig. 1 is obtained by modulating the 1.55-μm directly modulated DFB laser at a threshold current 18 mA with a sinusoidal input of 10 GHz. The lower and the upper sidebands represented by Eqs. (7) and (8) are shown in Fig. 1. It is observed that the first upper sideband amplitude is larger than the lower sideband amplitude, indicating modulation indices are in phase with each other.

Characterization of laser chirp

The small signal transfer function between frequency and intensity modulation of the distributed feedback laser is [20–23]

$$H(f) = \frac{\beta}{m}e^{ju} = \alpha\left(1 - j\frac{f_c}{f_m}\right) \quad (9)$$

where

$$f_c = \frac{\Gamma\varepsilon}{2\pi qV}(I - I_{th}) \quad (9a)$$

$$u = \tan^{-1}\left(-\frac{f_c}{f_m}\right) \quad (9b)$$

$$\frac{\beta}{m} = \frac{\alpha}{2}\sqrt{1 + \left(\frac{\Gamma\varepsilon}{2\pi qVf_m}(I - I_{th})\right)^2} \quad (9c)$$

where u is the phase factor, f_m is the modulation frequency, and f_c is the characteristic frequency or chirp frequency for which the adiabatic and the transient chirp have the same magnitude [24]. In the measurement technique, FM index (β) can be obtained from the average value of the upper and lower sideband amplitudes (($I_{+1} + I_{-1}$)/2), while the AM depth (m) can be obtained from their difference ($I_{+1} - I_{-1}$). In Fig. 2, the ratio of the FM response (β) to the AM response (m) is plotted against the modulation frequencies. The α-factor is extracted from Fig. 2(a), and the estimated value at a bias current of 50 mA is 4.32. The variation in the β/m ratio can also be used to evaluate the gain compression factor (ε), and the calculated value is 0.732 GHz/mA. Therefore, both α-factor and gain compression coefficient can be obtained from the measurements of the optical spectrum and the chirp is completely characterized. Again from Eq. (9), the nonlinear gain dominates for ($f_m < f_c$) and the β/m ratio becomes inversely proportional to the modulation frequency as shown in Fig. 2(a). For ($f_m > f_c$), *β/m saturates and becomes equal to* $\beta/m = \alpha/2$ and in this case linear gain dominates. Again, for $f_m = f_c$, Eq. (9c) becomes $\beta/m = \alpha/2^{1/2}$, implies the transition frequency at which adiabatic chirp and transient chirp have the same value. As seen in Fig. 2a, the β/m decreases with modulation frequencies but increases with bias current. This is because the characteristic frequency (f_c) increases with drive current shown in Fig. 2b. Figure 2b depicts that gain compression governs the characteristic frequency (f_c) as predicted by Eq. (9a). The gain compression governs the low-frequency part of the chirp, and its main function is to compress relaxation oscillation frequency through damping phenomenon. This decreases the transient part of chirp which governs a phase shift for the intensity transitions proportional to the rise and fall times. The chirp frequency or the characteristic frequency (f_c) represents the boundary between the transient and the adiabatic chirp. For modulation frequencies ($f_m < f_c$), adiabatic part of the chirp dominates and the transient chirp is overshadowed by the low-frequency chirp (adiabatic chirp).

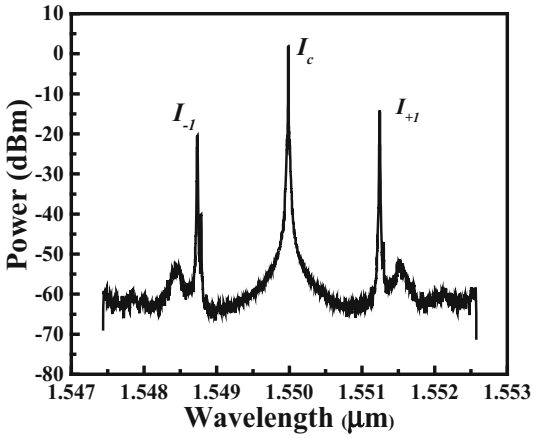

Fig. 1 Optical power spectrum of DFB laser modulated with a sinusoidal input of 10 GHz

Another most convenient approach for characterizing FM characteristics is to measure chirp-to-power ratio (CPR) derived in [25]. The chirp-to-modulated power ratio gives the optical frequency shift for a small signal modulated power and is defined as

$$\frac{\delta v}{\delta P} = \frac{\alpha}{2}\left(\frac{f_m}{P_0}\right) \quad (10)$$

where δv is the peak-to-peak optical frequency excursion, δP is the peak-to-peak power excursion, P_0 is the steady-state output power, and its value is 1.5 mV. To include the nonlinear gain compression, Eq. (10) should be multiplied by $[1 + (f_c/f_m)^2]^{1/2}$ suggested by [12, 13]. Under small signal approximation, we simulate modulation dynamics of a single-mode 1.55-μm DFB laser at a modulation speed of 5 Gbit/s, which allows us to evaluate chirp-to-power ratio. The power excursion and frequency excursion are obtained from the time variation of power and frequency, respectively, as shown in Fig. 3. Using Eq. (10), we obtain the

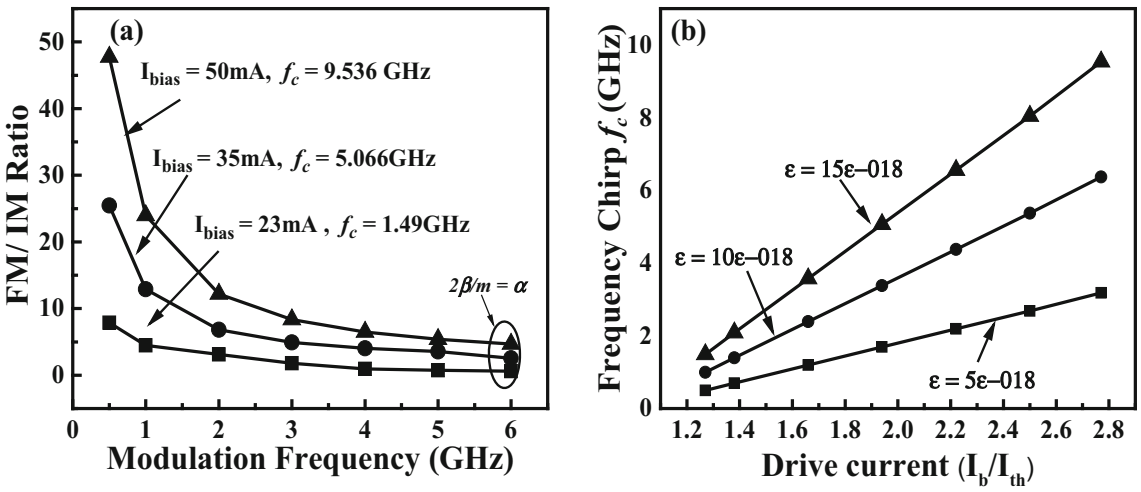

Fig. 2 Measured β/m ratio plotted against the modulation frequencies at different bias currents (**a**); calculated crossover frequency (f_c) plotted against the drive currents at various gain compression values (ε) (**b**)

value of α-factor equal to 4.162. Figure 4(a) shows the characteristic profile of the optical frequency spectrum at a bit rate of 5 Gbit/s. From Fig. 4(a), it is evident that adiabatic chirp is dominant with two peak frequencies corresponding to the 1's and 0's bits. The splitting of the carrier occurs because of the lower extinction ratio, i.e., Off state light level is non zero. From the frequency separation between the 1's and the 0's level, the adiabatic chirp coefficient (κ) can be deduced. It is more convenient to measure the adiabatic coefficient as a function of current rather than power [6]. Thus, for the laser spectrum shown in Fig. 4(a), the adiabatic chirp coefficient is 0.896 GHz/mA. From the adiabatic chirp coefficient, gain compression can be deduced equal to 3.9e−17. The splitting of the carrier signal is also present at a bit rate of 10 Gbit/s shown in Fig. 4(b). This produces the optical spectrum with enhanced transient chirp but did not eliminate the adiabatic chirp. The combined effect of the adiabatic and transient chirp produces asymmetrical optical spectrum with a plateau between '0' and '1' frequencies. This asymmetry depends on rising and falling edges of the input pulse, chirp factor and the power levels.

Large signal chirp

Both the FM/IM method and chirp-to-power ratio method are applicable to small signal modulation. For large signal modulation, the chirp is related to the optical output power, but the large signal dynamic response is highly complex due to nonlinear properties of the device. Rate Eqs. (1)–(3) can be used to model large signal version of chirp characteristics. In order to obtain the analytical solution to optical output power $P(t)$, the gain compression term in laser rate Eq. (2) is set to unity. Therefore, the effect of gain compression due to damping at high output power is ignored. Figure 5 shows the large signal response to an idealized step input drive current where P_{off} and P_{on} are the

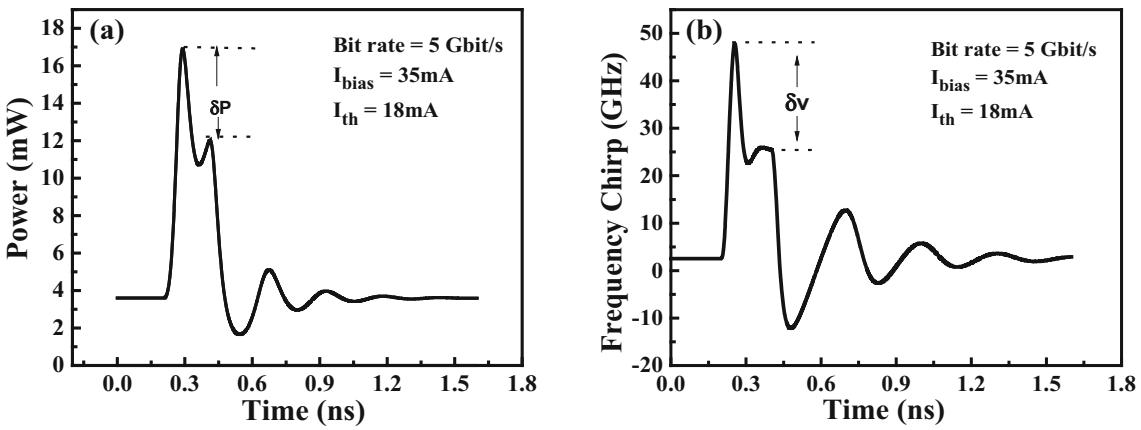

Fig. 3 Simulated waveforms of 1.55-μm DFB laser at 5 Gbit/s NRZ modulation for: time variation of power (**a**); time variation of frequency (**b**)

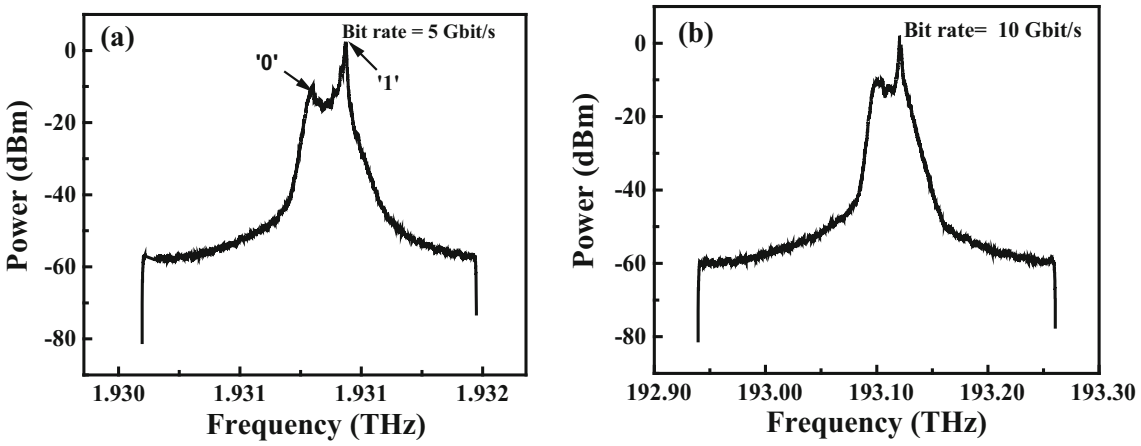

Fig. 4 Simulated spectrum of the reference laser [17] under NRZ modulation for: 5 Gbit/s with adiabatic chirp (**a**); 10 Gbits/s with adiabatic and enhanced transient chirp (**b**)

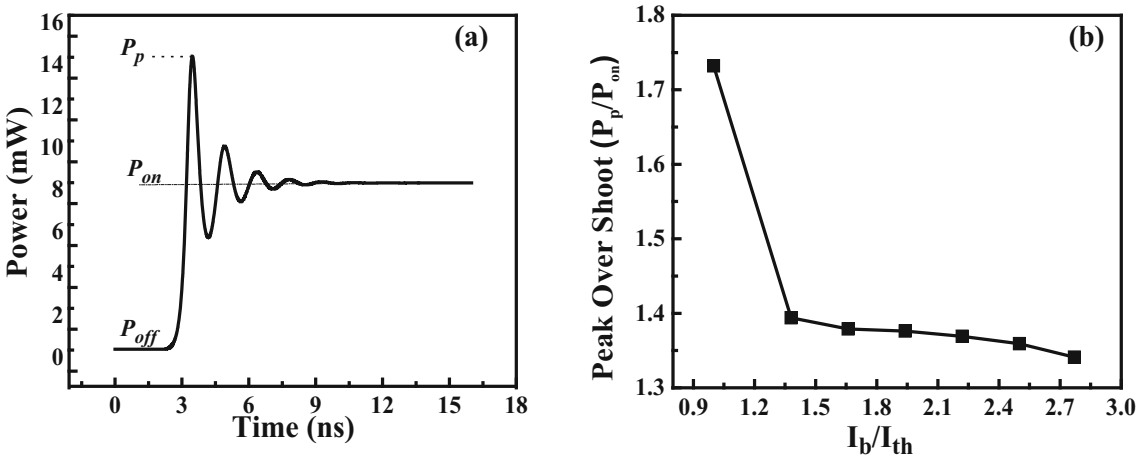

Fig. 5 Response of an idealized step input (**a**); peak power overshoot against the bias current (**b**)

corresponding values of I_{off} and I_{on}. P_p is the peak value of power overshoot. The chirp during the turn-on transients is given as [26]

$$\Delta v_{on} = \frac{\alpha\omega_{on}}{2\pi\sqrt{2}}\left[\ln\left(\frac{P_{on}}{P_{off}}\right)\right]^{1/2} \tag{11}$$

Equation (11) gives the turn-on transient chirp at $t = t_{on}$ and can be made smaller by reducing the On–Off ratio P_{on}/P_{off}. In this region, overshoot and ringing strongly effect the turn-on transient chirp. If the ringing is large, then there will be a strong chirp associated with the oscillations. Figure 5(b) shows the variation in peak overshoot with driving current. It is seen that as the drive current increases the peak over shoot decreases and improves the chirp behavior. Another approach to reduce the chirping overshoot is to simply increase the drive signal rise time. This significantly reduces the optical peak power overshoot and thus improves the chirp performance. Frequency chirp for the case of small signal modulation is related to modulation depth (m) as [27]

$$\Delta v = \frac{1}{4\pi}\alpha f_m m \tag{12}$$

Equation (12) is valid for small signal modulation as long as $m \ll 1$ and is not applicable when $m \geq 1$. Therefore, for large signal modulation, the frequency shift can be obtained from phase rate equation as:

$$\Delta v(t) = \frac{1}{2\pi}\left[\frac{d\phi}{dt}\right] \tag{13}$$

On solving for Eq. (1)– Eq. (4), we have

$$\Delta v(t) = \frac{\alpha}{4\pi}\left[\frac{d}{dt}\ln P(t) + \kappa P(t)\right], \tag{14}$$

This expression is large signal version of Eq. (12) and is independent of modulation depth (m). The magnitude of the first term in Eq. (14) is large during high-speed turn-on

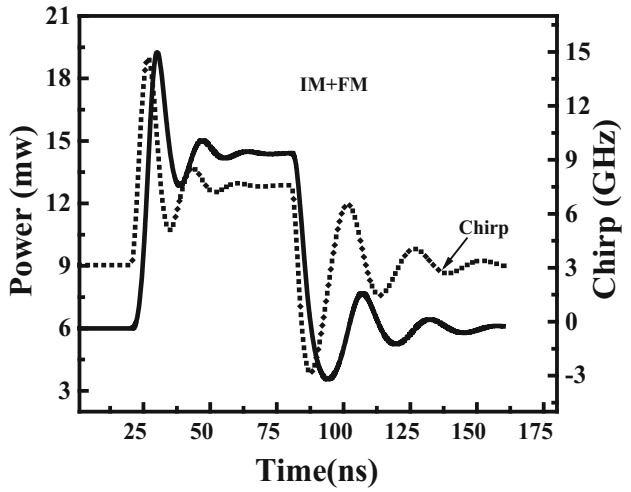

Fig. 6 Simulated time variation of power and frequency waveforms of 1.55-μm DFB laser at 5 Gbit/s NRZ modulation

and turn-off transients and oscillates between positive and negative values due to ringing. This term can be optimized by proper shape of the pulse to control the rate of change of $\ln P(t)$ [4]. This implies that devices with strong damping have good chirp characteristics due to reduction in the rate of change of $\ln P(t)$ after turn-on. The exact value of transient chirp depends on the details of pulse shape, e.g., using a Gaussian pulse shape $\exp(-t^2/T)$ gives $\Delta\nu = \alpha/2\pi T$ [24]. The second term in Eq. (14) corresponds to the adiabatic chirp (related to the frequency offset between the On and Off levels during modulation) arising from spontaneous emission and gain compression. Both the adiabatic chirp and transient chirp are modeled through time-resolved chirp measurements plotted in Fig. 6. It is observed that the chirp pulse starts earlier than the power pulse. Thus, there is a phase difference between them and the chirp parameters are calculated using chirp-to-power ratio (CPR) as discussed above.

Dispersion-tolerant system

It is well known that the laser chirp usually broadens the spectral bandwidth of the modulated optical signal and introduces performance degradation when the optical signal propagates through a dispersive media. The chirp controlled modulation or highly dispersion tolerant modulation comes from the phase correlative modulation between the adjacent bits. To realize the proper phase between the bits, directly modulated laser is biased at high bias current of $7I_{th}$. The advantages of operating the laser at high bias current are: high output power, high modulation bandwidth, suppression of side modes, low timing jitter and more importantly suppression of peak power overshoot, which in turn reduces the transient components in the optical output waveform. This makes the laser adiabatic chirp dominated and causes '1' bit blue-shifted relative to '0' bit. The π out of phase between the adjacent bits is the key to the dispersion tolerance [28]. For 5 Gbit/s modulation rate, the pulse width is 0.2 ns, in order to get π phase shift, the adiabatic chirp needed to be equal to 2.5 GHz; this implies that '1' bit has 2.5 GHz blue shift relative to '0' bit. Therefore, proper adiabatic chirp can be generated by adjusting the laser parameters and the bias conditions to achieve a AM-to-FM conversion. (i.e., '1' is blue-shifted compared to '0' bit). This results in low extinction ratio, which can be rectified using proper optical filter. According to the analysis of the chirp model, we perform multi-parameter sweeping to optimize the laser structure, which is suitable to get π out of phase between the On and Off states of the DFB laser for the transmission of directly modulated signals. The extracted parameters are shown in Table 1.

Simulated results for the time variation power and frequency at the output of the laser biased at 60 mA with peak modulation current of 28 mA are shown in Fig. 7. These results are based on the internal states of the laser rate equation model. As seen, the ringing effect related to the transient chirp is considerably reduced due to strong

Table 1 Extracted parameter values for adiabatic chirp dominated laser

Parameters	Initial estimation	Extracted parameters
Active layer volume (cm^3)	1.98e+011	1.62e−011
α-Factor	5	4.62
Differential gain coefficient (cm^2)	1.19e−015	1.12e−015
Mode confinement factor	0.22	0.19
Transparent carrier density (cm^{-3})	1.07e+018	0.31e+018
Carrier lifetime (ns)	0.79	0.158
Photon lifetime (ps)	0.8	3.13
Spontaneous emission factor	1e−004	36e−006
Gain compression factor (cm^3)	1.43e−017	3.9e−017

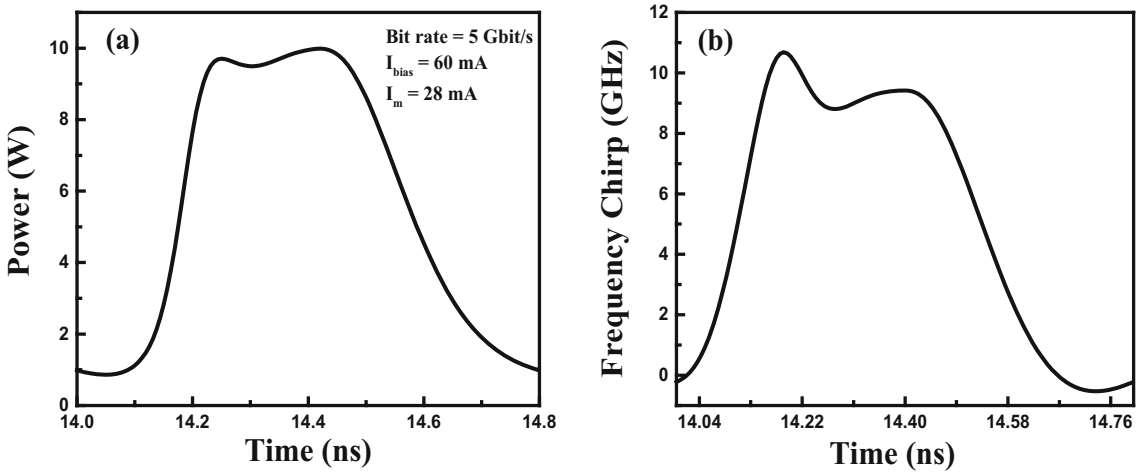

Fig. 7 Simulated time-resolved chirp of a directly modulated DFB laser at 5 Gbit/s modulation with NRZ modulation technique for: time variation of power (**a**); time variation of frequency (**b**)

damping and the optical output power is observed as the key to the AM-to-FM conversion via adiabatic chirp.

Conclusion

Based of the single-mode laser rate equations, we investigate the laser chirp characteristics of a 1.55-μm directly modulated DFB laser by simulation. The laser parameters affecting the chirping effect are: gain compression and α-factor. The transient chirp is affected by α-factor, and the adiabatic chirp is affected by both the gain compression and the α-factor. Measurements of the chirp parameters using transfer function and the chirp-to-modulated power ratio are presented. We have identified that the characteristic frequency (f_c) represents the boundary between the adiabatic and transient chirp. The time variation of power and frequency of an optical signal, using time-resolved chirp technique, is used for the characterization of large signal chirp. Finally, directly modulated laser with suitable chirp is generated by operating the laser at high bias current, suppressing transient components and making the laser adiabatic chirp dominant. Therefore, proper adiabatic chirp can be generated by adjusting the laser parameters and the bias conditions to achieve an AM-to-FM conversion.

References

1. I. Tomkos, I. Roudas, R. Hesse, N. Antoniades, A. Boskovic, R. Vodhanel, Extraction of LRE parameters for simulation of metropolitan area transmission systems and networks. Opt. Commun. **194**, 109–129 (2001)
2. J.M. Tang, K.A. Shore, 30 Gb/s signal transmission over 40 km directly modulated DFB laser based single mode fiber links without optical amplification and dispersion compensation. J. Lightw. Technol. **24**(6), 2318 (2006)
3. K. Czotsher, S. Weisser, A. Leven, J. Rosenzweig, Intensity modulation and chirp of 1.55 μm multiple-quantum-well laser diodes: modeling and experimental verification. IEEE J. Sel. Top. Quantum Electron. **5**(3), 606–612 (1999)
4. A. Yousuf, H. Najeeb, Effect of gain compression above and below threshold on the chirp characteristics of 1.55 μm DFB laser. Opt. Rev. **23**(6), 897–906 (2016)
5. I. Tomkos, Demonstration of negative dispersion fibers for DWDM metropolitan networks. IEEE J. Sel. Top. Quantum Electron. **7**, 439–460 (2001)
6. B.W. Hakki, Evaluation of transmission characteristics of chirped DFB lasers in dispersive optical fiber. J. Lightw. Technol. **10**(7), 964–979 (1992)
7. C.D. Campos, P.R. Horche, A.M. Mínguez, Interaction of semiconductor laser chirp with fiber dispersion: impact on WDM directly modulated system performance, in *The Fourth International Conference on Advances in Circuits, Electronics and Micro-electronics* (2011). ISBN: 978-1-61208-150
8. S. Yamamoto, M. Kuwazuru, H. Wakabayashi, Y. Iwamoto, Analysis of chirp power penalty in 1.55 μm DFB-LD high speed optical fiber transmission systems". J. Lightw. Technol. **5**(10), 1518–1524 (1987)
9. H. Gysel, M. Ramachandra, Electrical predistortion to compensate for combined effect of laser chirp and fibre dispersion. Electron. Lett. **27**(5), 421–423 (1991)
10. R. Hui, A. Mecozzi, A.D. Ottavi, P. Spano, Novel measurement technique of alpha factor in DFB semiconductor lasers by injection locking. Electron. Lett. **26**(14), 997–998 (1990)
11. C. Henry, Theory of the linewidth of semiconductor lasers. IEEE J. Quantum Electron. **18**(2), 259–264 (1982)
12. M. Osinski, Linewidth broadening factor in semiconductor laser. IEEE J. Quantum Electron. **23**(11), 09–29 (1987)
13. T.L. Koch, R.A. Linke, Effect of nonlinear gain reduction on semiconductor laser wavelength chirping. Appl. Phys. Lett. **48**(10), 613–615 (1986)
14. A. Hamgauer, G. Wysocki, Gain compression and linewidth enhancement factor in mid-IR quantum cascade lasers. IEEE J. Quantum Electron. **21**(6), 1200411 (2015)
15. G. Wang, R. Nagarajan, D. Tauber, J. Bowers, Reduction of damping in high speed semiconductor lasers. IEEE Photonics Technol. Lett. **5**(6), 642–645 (1993)

16. L. Koch, R.A. Linke, Effect of nonlinear gain reduction on semiconductor laser wavelength chirping. Appl. Phys. Lett. **48**(10), 613–615 (1986)
17. J.C. Cartledge, R.C. Srinivasan, Extraction of DFB laser rate equation parameters system simulation purposes. J. Lightw. Technol. **15**(5), 852–860 (1997)
18. G.P. Agrawal, N.K. Dutta, *Semiconductor Lasers*, 2nd edn. (Van Nostrand Reinhold, New York, 1993)
19. S. Kobasyashi, Y. Yamamoto, M. Ito, T. Kimura, Direct frequency modulation in AlGaAs semiconductor lasers. IEEE J. Quantum Electron. **30**(4), 428–441 (1982)
20. A. Villafranca, J. Lasobras, I. Garces, Precise characterization of the frequency chirp in directly modulated DFB lasers, in *Proceedings of Spanish Conference Electron Devices* (2007), pp. 173–176
21. T. Zahang, N.H. Zhu, Measurement of chirp parameter and modulation index of a semiconductor laser based on optical spectrum analysis. IEEE Photonics Technol. Lett. **19**(4), 227–229 (2007)
22. K. Kechaou, F. Grillot, J.G. Provost, B. Thedrez, D. Erasme, Self injected semiconductor distributed feedback laser for frequency chirp stabilization. Opt. Express **20**(23), 26062–26074 (2012). https://doi.org/10.1364/OE.20.026062
23. L. Bjerkan, A. Royset, L. Hafskjaer, D. Myhre, Measurement of laser parameters for simulation of high speed fiberoptic systems. J. Lightw. Technol. **14**(5), 839–850 (1996)
24. R.C. Srivasana, J.C. Cartledge, On using fiber transfer function to characterize laser chirp and fiber dispersion. IEEE Photonics Technol. Lett. **7**(11), 1327–1329 (1995)
25. T.L. Koch, J. Bowers, Nature of wavelength chirping indirectly modulated semiconductor lasers. J. Electron. Lett. **20**(25/26), 1038–1040 (1984)
26. R.S. Tucker, High-speed modulation of semiconductor lasers. J. Lightw. Technol. **3**, 1180–1192 (1985)
27. G.P. Agrawal, N.K. Dutta, *Long Wavelength Semiconductor Lasers* (Van Nostrand Reinhold Co., New York, 1986)
28. D. Mahgerefteh, Y. Matsui, X. Zheng, K. McCallion, Chirp managed laser and applications. IEEE J. Sel. Top. Quantum Electron. **16**(5), 1126–1139 (2010)